

The G0 Target LH2 No Beam Tests

Silviu Covrig
Kellogg Radiation Laboratory
Caltech
silviu@krl.caltech.edu
June 2002

Introduction

The G0 target system was installed in Hall C at JLab during the months of April and May, 2002. The target service module has been installed on the G0 Superconducting Magnet. The gas panel that services the target has been installed in Hall C, along with the electronics for target monitoring and controls. After the target installation was completed a series of checks were done on the system and the target was declared leak tight and ready for commissioning without beam. First, the target had to pass the so called Safety Neon Test, consisting of liquefying Neon, filling the target and a subsequent boiloff triggered by a break in the vacuum with a source of dry Nitrogen. The target successfully passed this test on May 29, 2002. Second, the target had to undergo a series of tests with liquid Hydrogen. This document describes the G0 target performance with liquid Hydrogen *in situ* and with no beam. The purpose of these tests was to determine the performance of the target with liquid Hydrogen using ESR's 15 K Helium coolant supply. This was also the very first time we had liquid Hydrogen in the target and gained experience with running an LH₂ G0 target.

The G0 Target System

The target system is described in detail in the **PDD** [1]. In short the G0 target system is made of:

- Cryogenic loop:
 - Pump, target manifold, heat exchanger, heaters;
- Gas handling system:
 - Gas panel, ballast tank, gas transfer lines;
- Controls:
 - Target computer, electronics, P-T sensors, software controls;

While we do not read the pressure directly on the cryogenic loop, but on the gas panel, the loop is instrumented with six temperature sensors immersed in the target fluid, one pair across the cryogenic pump and the high power heater, one pair across the heat exchanger and one pair across the target manifold. We can also read the coolant temperature in three points, before the JT valve and right across the heat exchanger. On the gas panel we have the capability of reading and monitoring the pressures in the system: the pressure in the loop, the pressure in the Helium cell, the differential pressure across the exit window of the Helium cell and the differential pressure across the cryogenic pump. As a separate instrumentation from the gas panel we also monitor the pressure in the ballast tank. The target control computer runs a combination of StripTool and MEDM GUIs that read back and display the target parameters. A VME crate containing an Input-Output Controller is situated in an electronics rack in the Hall and takes care of the low level software control of the target. The data from the IOC is sent to the target computer via Ethernet and displayed on the target computer screen. During data acquisition running the target operator monitors and responds to target related problems in the Hall C counting house. For the whole period of time during the tests described here

the cryogenic pump, the high power heater and the JT valve were controlled from the target computer. More about the controls for the G0 target can be found out in ref. [2].

Description of the tests

In chronological order the tests done with the target were:

- Pump test
- Flow measurement in the loop
- Heat exchanger performance
- Reliability run
- IOC crash and recovery tests

Besides these more or less standard tests that assess the performance of a cryogenic target, a different kind of test for us was liquefying Hydrogen for the first time in this target.

After the target passed the Safety Neon Test on May 29, we prepared the target for Hydrogen. The cooldown with Hydrogen started on June 3 round 10 am from 291 K/ 24 psig gaseous H₂ in the loop, using about 4 g/s He coolant from the 15 K ESR coolant supply. The cooldown process occurred parasitically since the Hall A target was full of LH₂. Liquefaction started at 11:10 am at 24 K / 23.3 psig. The mysterious bump in the coolant happened when we switched from warm return to the cold return of the coolant. We managed to keep the target round 24 K until the Hall A target recovered from it (it took about 40 min). The target was declared full with LH₂ at 1:30 pm at 23.4 K, and at 2 pm we had the target 3 K subcooled liquid at a final point in the P-T space of 14.7 psig and 20.3 K. Hydrogen consumption from the ballast tank was an estimated 10 psig, the liquid volume is 6.5 liters and the liquid mass is 0.47 kg. Please see fig. 3, 4 and 5 for a closer look at the cooling down process.

For the rest of the day we did the pump studies. The next day, during the day shift, we did the flow measurements in the loop and the heat exchanger performance measurements at four cryogenic pump frequencies. In the afternoon we checked the PID control of the high power heater and found some nominal PID parameters. After that we restored the nominal frequency of the pump, 30 Hz, and left the high power heater on PID control for the remaining of the week, which accounted for reliability test. On June 7 we did the IOC power off/on and recovery test and ultimately boiled the target and parked it with Helium at room temperature.

1. Pump flow studies

To determine the pump flow and to assess the heat exchanger performance we followed ref. [3]. For flow studies we measured the temperature difference across a known heat source at four different frequencies, and from this the mass flow can be determined with:

$$\eta \cdot \dot{Q}_H = \dot{m}_{LH_2} \cdot c_P \cdot (T_{PO} - T_{PI}) \quad (1)$$

where \dot{Q}_H is the power delivered by the high power heater power supply and $\eta \cdot \dot{Q}_H$ is the power deposited by the high power heater into the loop. The η factor accounts for the

source of physical losses, the power loss into the electrical transfer lines between the high power heater power supply and the heater itself. The logged parameter was the power delivered by the power supply. To get the power deposited into the loop, the η factor was computed to be 0.75.

We took data at four different cryogenic pump rotational frequencies: 10, 20, 30 and 40 Hz, and at six different heater power values: 550, 450, 350, 250, 150 and 50 W for each frequency. The specific isobaric heat and density for liquid Hydrogen were corrected for temperature dependence. Since the pressure stayed the same during these studies, there were no pressure related corrections to the input Hydrogen parameters. At each power value the data included in the computation of the mass rate was the closest to the Thermodynamic equilibrium. With this data one can also estimate the pump efficiency with the formula:

$$\epsilon_P = \frac{\eta}{c_P(T) \cdot \rho(T) \cdot V_s \cdot f} \cdot \frac{\dot{Q}_H}{T_{PO} - T_{PI}} \quad (2)$$

where V_s is the theoretical volume displacement of the cryogenic pump in one revolution. We are using a vane-axial pump with two identical impellers. Each impeller is equipped with three blades. The estimate for V_s , taking into account the volume of the blades, is 0.198 liters. The rotational frequency of the cryogenic motor shaft is denoted by f . The motor has attached rigidly to its shaft a permanent magnetic dipole, which rotates along with the shaft. A Cu coil sits inside the upstream conical flow diverter and faces the dipolar magnet. This assembly constitutes what we call the tachometer. Whenever the motor's shaft rotates an AC electrical signal is induced by the magnet into the coil and read back by a frequency enabled DMM, Agilent 34401A. In this setup the frequency readback is completely independent from the cryogenic pump controller itself.

With the differential pressure across the cryogenic pump one can determine the torque of the cryogenic motor at different frequencies, but since traditionally one displays the differential pressure, a final torque graph is not included in this report, but the relation between torque and pressure is:

$$\tau = \frac{V_s \cdot \Delta p}{2\pi} \quad (3)$$

The mechanical power delivered by the cryogenic pump can be determined from the data with:

$$P = \epsilon_P \cdot V_s \cdot f \cdot \Delta p \quad (4)$$

2. Heat exchanger studies

The heat exchanger used in the G0 target is a counterflow heat exchanger with finned tubing. There are two coils in parallel, through the inner of the coils circulates cold He gas from the 15 K He supply at the ESR, and around the finned tubing circulates LH₂. There is a flow diverter inside the heat exchanger made of solid Al that forces the liquid

to go around the fins only. For a counter flow heat exchanger, like the one in the G0 target, the mean temperature difference is given by:

$$\Delta T_{LM} = \frac{T_{ho} - T_{ci} - (T_{hi} - T_{co})}{\log\left(\frac{T_{ho} - T_{ci}}{T_{hi} - T_{co}}\right)} \quad (5)$$

and the heat exchanger coefficient is given by:

$$U = \frac{\dot{q}_{He}}{\Delta T_{LM}} = \frac{\dot{m}_{He} \cdot c_p^{He} \cdot (T_{co} - T_{ci})}{\Delta T_{LM}} \quad (6)$$

where T_{hi} is the temperature of the LH₂ going into the heat exchanger and T_{co} is the temperature of the He coolant going out of the heat exchanger, for example. During the heat exchanger studies the coolant mass flow as read from the ESR flowmeter for the 15 K supply for Hall C never exceeded 10.5 g/s. Like in the pump studies ΔT_{LM} was determined for four cryogenic pump frequencies and six setpoints for the high power heater.

To characterize the heat exchanger further we also determined its effectiveness, which for a counter flow heat exchanger is defined theoretically as:

$$\epsilon_{HX}^{th} = \frac{1 - e^{-N \cdot (1-R)}}{1 - R \cdot e^{-N \cdot (1-R)}} \quad (7)$$

where R is the heat capacity rate ratio, and N is the number of heat transfer units, defined as:

$$R = \frac{(\dot{m} \cdot c_P)_{min}}{(\dot{m} \cdot c_P)_{max}}, \quad N = \frac{U}{(\dot{m} \cdot c_P)_{min}} \quad (8)$$

where *min/max* refer to the coolant and/or liquid.

Physically it represents the ratio between the actual rate of heat transfer in the heat exchanger and the maximum allowable rate by the second law of Thermodynamics. Experimentally the value of the effectiveness is given by:

$$\epsilon_{HX}^{exp} = \frac{T_{co} - T_{ci}}{T_{hi} - T_{ci}} \quad (9)$$

Results and discussions

There are two sets of graphs with results from these studies attached. For cryogenic pump efficiency and flow measurements in the loop the big error bars are coming from the fact that LH₂ is not the best choice for determining these parameters for a cryogenic pump because of the small temperature differences that can be induced across the high power heater, on average about only four times bigger than the systematic error that the temperature sensors were calibrated by the vendor, 25 mK. With the present controller the cryogenic pump torque saturated at about 42 Hz shaft frequency. The saturation is not achieved on a differentiable curve, which means that it is not caused by the motor torque reaching its highest physical

limit, but by the controller reaching its current limit. It may as well be that a better controller could solve the problem and turn the shaft under load at higher frequencies. At the saturation torque, of 23 oz-in, with the present controller, the cryogenic pump head was 0.75 psid, and the mechanical power delivered to the liquid was 43 W. The rating from the motor manufacturer is for 50 oz-in at the nominal frequency of the cryogenic pump of 30 Hz. The power delivered by the pump is fitted very well by a polynomial of third degree in frequency, but the pump head is not by a second degree polynomial in frequency, which means that the pump efficiency is frequency dependent, as observed. The mass flow seems to be maximum at the G0 nominal frequency of 30 Hz, with a pump efficiency of 0.59. At 20 Hz the pump efficiency gets close to the efficiency limit for vane-axial pumps of 0.8.

The heat exchanger was able to remove 450 W of heat from the loop with a coolant flow of 10.5 g/s from the 15 K coolant supply from the ESR, and this by sharing the supply with a full LH₂ target in Hall A. The flow of the coolant, as read from the ESR flowmeter, is said to be good to within 30%. There were no calls from the ESR the whole week about excess coolant usage in Hall C for the G0 target, although we share the 15 K coolant supply with Hall A cryogenic target.

The heat transfer coefficient, U, as computed from the semiempirical formula:

$$\frac{1}{U} = \frac{1}{(h_{He} \cdot A_{He})} + \frac{1}{(h_{LH_2} \cdot A_{LH_2})} \quad (10)$$

where A is the area for heat transfer on He/LH₂ side respectively and:

$$h = 0.023 \cdot \frac{C_P \cdot G^{0.8} \cdot \eta^{0.2}}{D_e^{0.2} \cdot Pr^{0.6}} \quad (11)$$

where G is the mass flow per unit area of the flow, η is the fluid viscosity, D_e is the wetted perimeter and Pr is the Prandl number for the fluid,

for the nominal running conditions at a cryogenic pump speed of 30 Hz is 285 W/K. In the same running conditions the data yielded a value for the heat transfer coefficient of 150 W/K. Not a good agreement at all, but not unexpected. The model computed value for U assumes that the temperature is constant across the fins, while in reality it is a gradient from the Helium side to the tip of the fins, and the gradient varies along the heat exchanger. Also, originally the heat exchanger had nylon rope wrapped around the fin tubing to force the liquid Hydrogen flow to go around the fins, but it was removed by Cathleen Jones for fear that it may block the flow on the Hydrogen side, and because of this the heat exchanger has some leakage that depends on the flow speed and has the effect of reducing the value of the heat transfer coefficient from what you'd get from (10-11).

The mean temperature difference across the heat exchanger, ΔT_{LM} has the expected behavior in frequency, it decreases with the increase in pump frequency, but it is not straight at high rotational frequencies of the cryogenic pump and high heat loads which is also related to the leakage. The effectiveness is very close to the theoretical estimate for a counter flow heat exchanger, for $N > 3$ it should be above 0.95. In our heat exchanger the number of heat transfer units is at least 3.55, and the measured effectiveness is above 0.98 for pump frequencies higher than 30 Hz.

The reliability run was finished uneventfully. From the IOC crash and recovery test, actually a power *off/on* test, we decided to move the cryogenic pump control from computer to manual only. The PID feedback control of the high power heater proved to be very reliable and fast in tracking the heat load in the loop. The feedback keeps a temperature sensor at a constant value. Although the feedback works fine on its own we decided to implement a slightly different feedback loop in which the beam power is subtracted from the total heat load to the target and the rest of it is fed to the high power heater. In this way the PID loop will be managing a lower power budget on the high power heater with beam current variations and beam *on/off* states and we'll have a better control of the thermodynamic instabilities associated with the beam. Based on this experience we decided that the low power heater is not needed to control the temperature in the loop and it will not be used, unless future experience will prove it necessary.

When we boiled the target, after the IOC tests, we didn't realize that the target logger stopped running when we power cycled the target computer and we lost that data. The boiloff occurred without incident, as expected, anyway.

After we boiled the liquid, when the cryogenic loop was at about 50 K, cold Hydrogen gas, we did a pump frequency scan and the pump ran up to 73 Hz. From this running frequency when the controller was powered off the shaft stopped turning in 23 seconds, meaning that there is no significant friction impeding the rotation.

In the end it was a very successful week for the target. We accumulated data with liquid Hydrogen for the first time, and along we gained operational experience with running the G0 target with LH₂. The target was monitored round the clock from the Hall C counting house in the same conditions it would during a normal running experiment with beam. In the end it was concluded that the target commissioning without beam finished and that the target passed all the required pre-beam tests. The G0 target was declared ready for commissioning with the G0 beam.

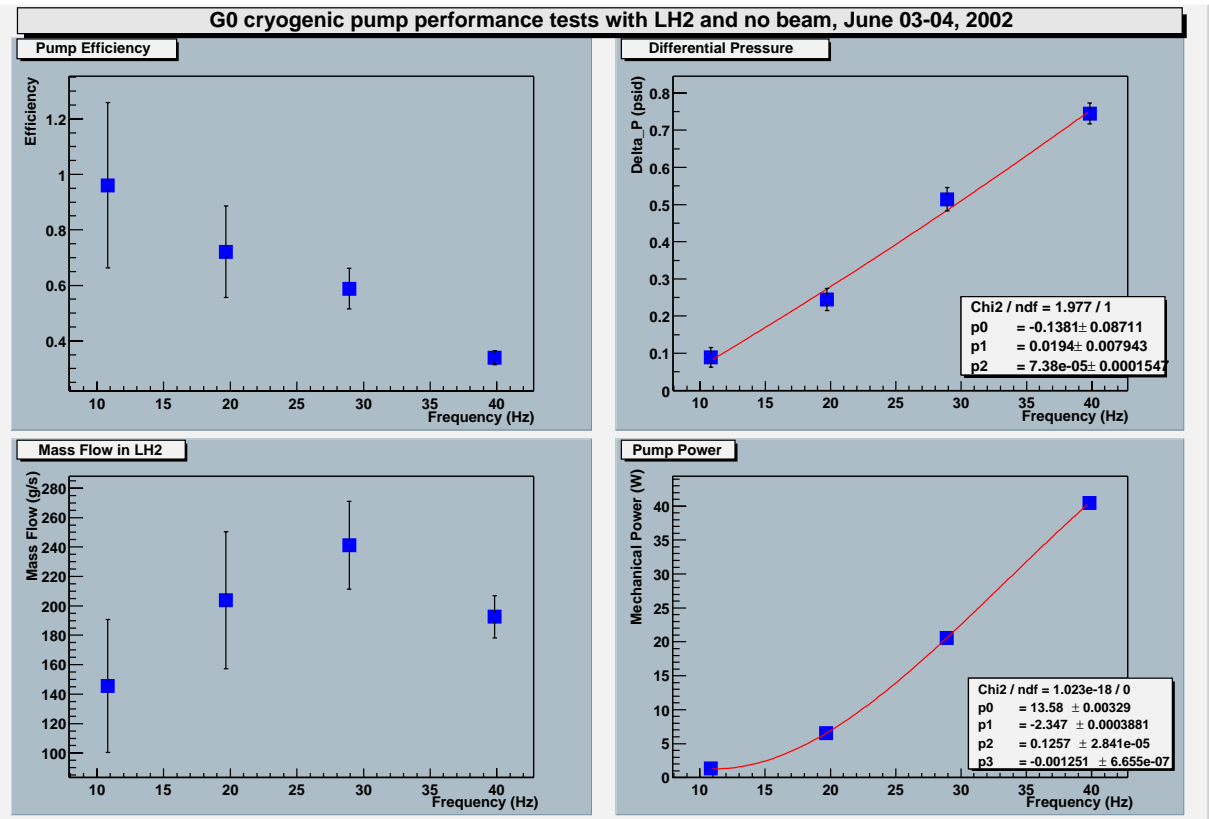


Figure 1: Cryogenic Pump Studies

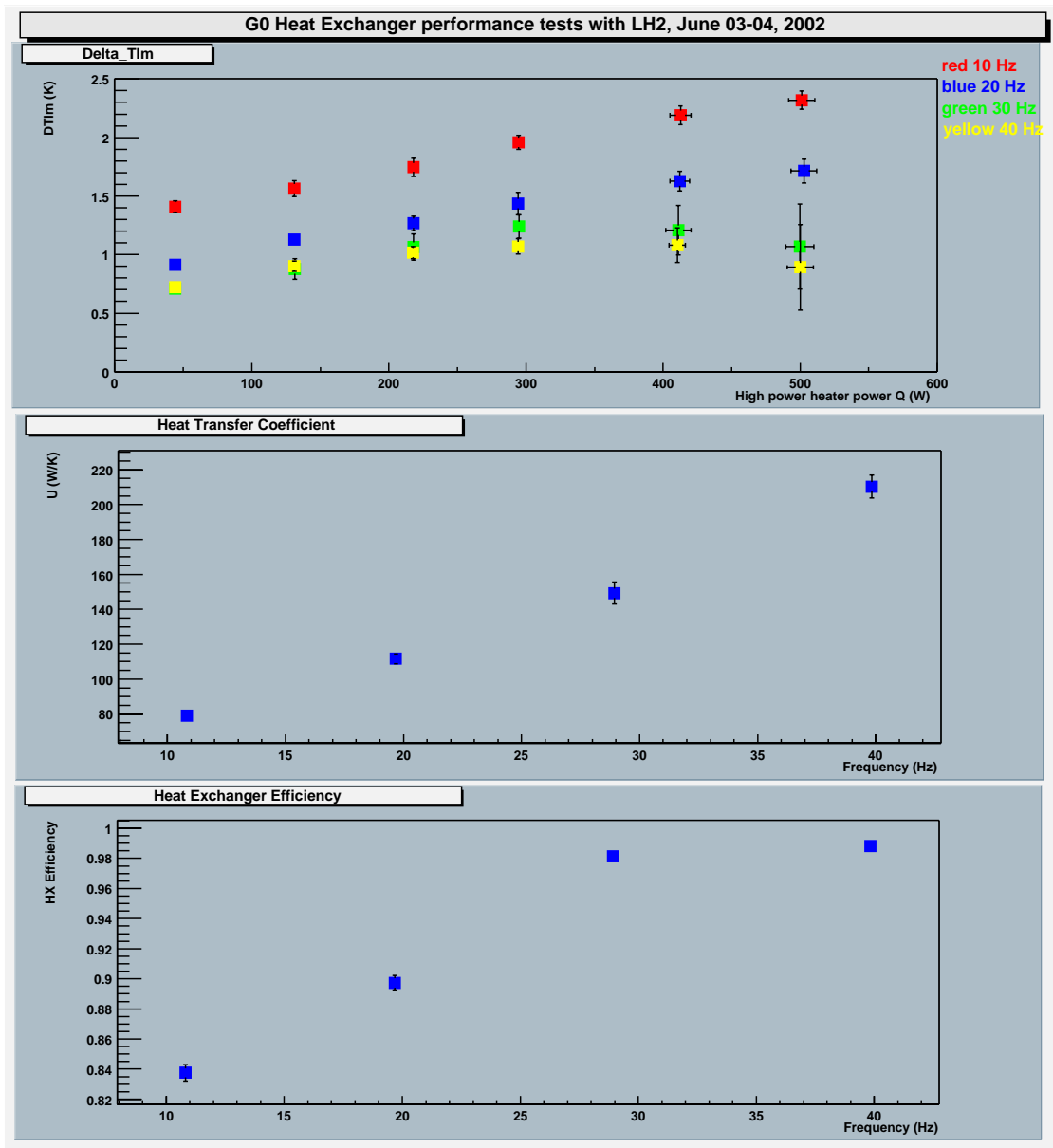


Figure 2: Heat Exchanger Studies

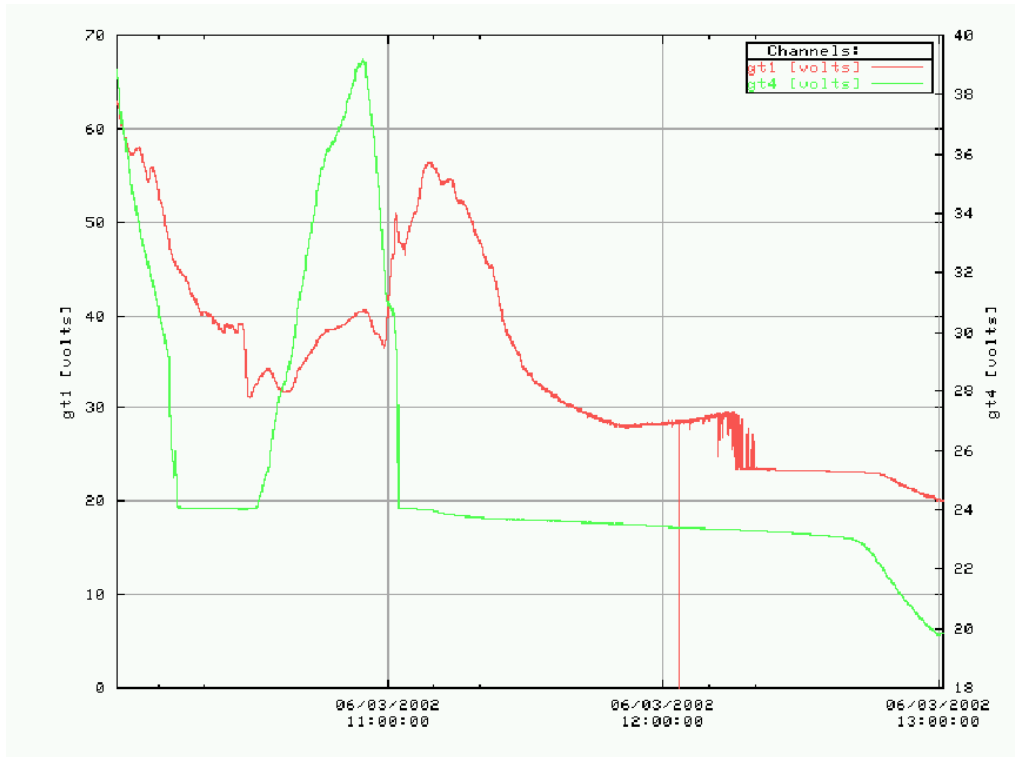


Figure 3: The liquefaction of Hydrogen as seen from the point of view of two temperature sensors in the loop: gt1, the one downstream of the cryogenic pump, the only one in the loop sitting above the horizontal plane, which dictates when the loop gets full of liquid; and gt4, the temperature sensor sitting upstream of the target cell manifold. One can see that when the loop gets full with LH₂, gt1 drops on the liquid temperature. The figure also displays the subcooling process of the liquid by 3 K.

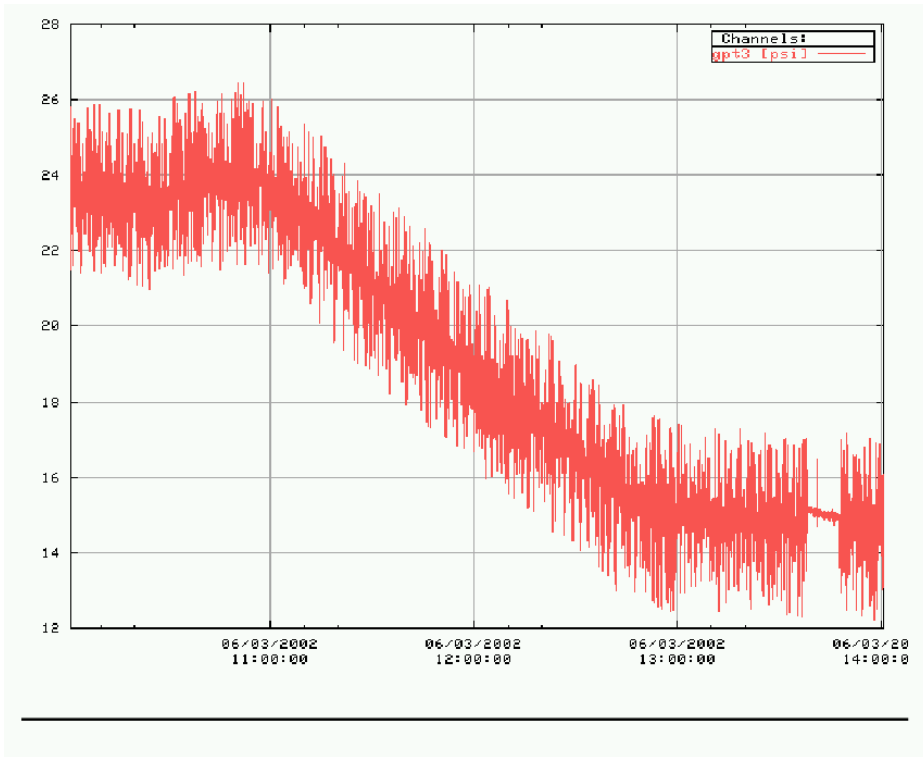


Figure 4: The liquefaction of Hydrogen as seen from the point of view of the pressure in the cryogenic loop, gpt3. Starting point is at about 24 psig, ending point is at about 14.7 psig in the 3 K subcooled liquid state. The noise on the signal comes from the cryogenic pump controller. Latter instrumentation of the pressure signals with RC filters cleaned the signals quite a lot, they look now like the temperature signals.

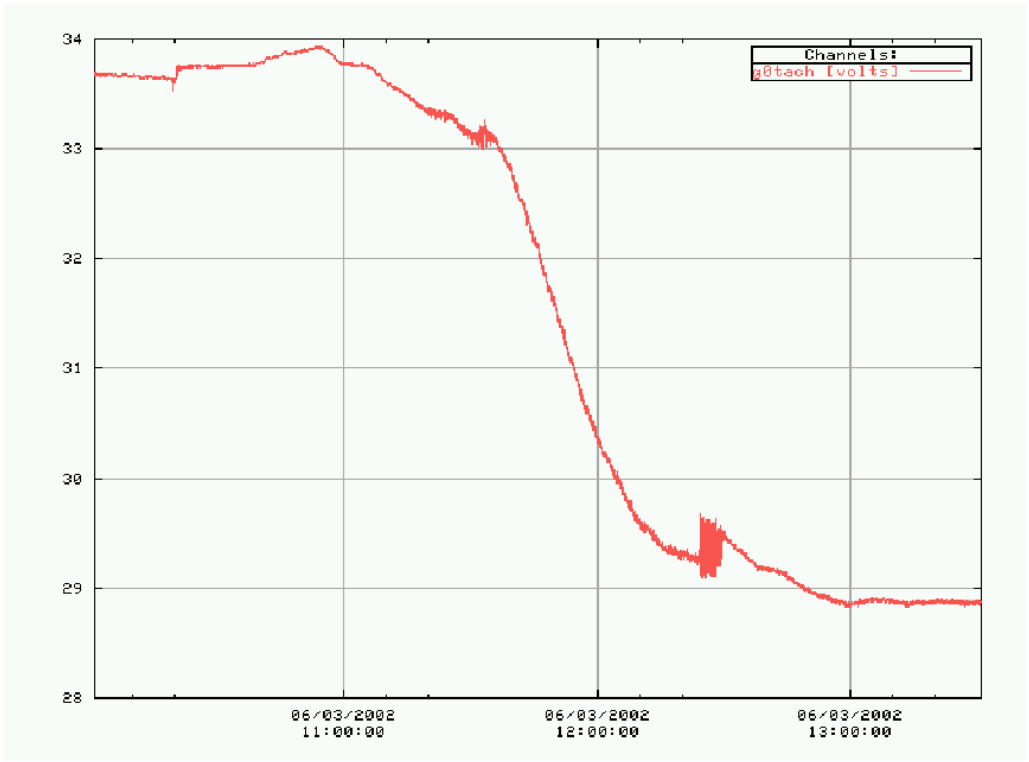


Figure 5: The liquefaction of Hydrogen from the point of view of the rotational speed of the cryogenic pump. One can see the reduction of the speed as the load increases with the liquid level, and the settling of the speed when the pump gets engulfed by the liquid.

Bibliography

- [1] C. E. Jones and E. J. Beise, “*G0 Liquid Hydrogen Target Preliminary Design Document*”, November 25, 1998
- [2] E. J. Beise et al., “*The G0 Target Controls Manual*”, last version October 21, 2002
- [3] E. J. Beise et al., Nucl. Instrum. Meth. **A 378**, 383 (1996)